# Effect of impurities on the growth of {113} interstitial clusters in silicon under electron irradiation

K. Nakai[1], K. Hamada[1], Y. Satoh[2] and T. Yoshiie[3]

[1] *Faculty of Engineering, Hokkaido University, Sapporo 060-8528, Japan*
[2] *Institute for Materials Research, Tohoku University, 2-1-1 Katahira, Aoba-ku, Sendai 980-8577, Japan*
[3] *Research Reactor Institute, Kyoto University, Kumatori-cho, Sennan-gun, Osaka 590-04, Japan*

*(Received ; final version received )*

The growth and shrinkage of interstitial clusters on {113} planes were investigated in electron irradiated Cz-Si, Fz-Si, and impurity-doped Fz-Si (HT-Fz-Si) using a high voltage electron microscope. In Fz-Si, {113} interstitial clusters were formed only near the beam incident surface after a long incubation period, and shrank on subsequent irradiation from the backside of the specimen. In Cz-Si and HT-Fz-Si, {113} interstitial clusters nucleated uniformly throughout the specimen without incubation, and began to shrink under prolonged irradiation at higher electron beam intensity. At lower beam intensity, however, the {113} interstitial cluster grew stably. These results demonstrate that the {113} interstitial cluster cannot grow without a continuous supply of impurities during electron irradiation. Detailed kinetics of {113} interstitial cluster growth and shrinkage in silicon, including the effects of impurities, are proposed. Then, experimental results are analyzed using rate equations based on these kinetics.

Keywords: Cz silicon; Fz silicon; point defects; interstitial clusters; irradiation damage; electron irradiation; impurities

## 1. Introduction

The electronic properties of silicon are highly sensitive to point defects and impurities. Although many studies have been performed, several aspects of the behavior of point defects and impurities are not well understood [1]. High energy electron irradiation experiments using a high voltage electron microscope (HVEM) are one of the most powerful techniques for the investigation of point defect processes in silicon, since the point defect production rate is high and the direct observation of point defect clusters is possible.

Since the first observation of small defects clustered in silicon by Thomas [2] after electron irradiation using HVEM, many papers have been published. The

following important results were obtained. Many of the point defect clusters formed during electron irradiation between 35 K to 923 K are rod-like clusters on {113} planes elongated in the <110> direction [3-9]. These clusters are interstitial-type [5, 7-9]. The atomic structure of the clusters were determined by high resolution electron microscopy [10] and energy calculations [11-13]. The effect of impurities is important for the cluster formation [14]. In Czochralski grown silicon (Cz-Si), {113} interstitial clusters are formed immediately after electron irradiation at high temperatures (573-673 K), and appear homogeneously throughout the matrix. In floating-zone silicon (Fz-Si), {113} interstitial clusters nucleate and grow only near the electron incident surface, after a long incubation period [9]. This difference is due to pre-existing oxygen impurities in Cz-Si. The incubation period for cluster nucleation in Fz-Si originates from the time required for the accumulation of implanted impurities under electron irradiation. The effect of other impurities, such as carbon, on the nucleation of clusters was also examined [8, 15-19]. Impurities play an important role in both the growth and nucleation of defect clusters [8,17,19-22]. For example, Bean *et al*. [22] reported the removal of oxygen and carbon from unperturbed lattice sites with increasing electron irradiation dose. Aseev *et al*. [8] concluded that {113} clusters formed at 973 K were precipitates, which contained oxygen, carbon, and interstitial silicon.

Goss *et al*. presented the results of first-principals calculations of the structure and energetics of interstitial cluster candidate structures on the {111}, {113}, and {001} planes [13]. They concluded that the most stable plane was {111}, and not {113}. There is a strong possibility that impurities stabilize the {113} structure.

Shrinkage and annihilation of the {113} interstitial clusters and the formation of new {113} interstitial clusters during irradiation were observed in several cases.

The {113} interstitial clusters formed in the matrix of Cz-Si [16] and carbon-doped Fz-Si [15] shrank, and new clusters formed near the beam incident surface during prolonged irradiation. Interstitial clusters that formed near the beam incident surface in Fz-Si [23] and in boron- or phosphorus- implanted Cz-Si [24] also shrank on re-irradiation after the specimen had been reversed. Oshima *et al*. [16] attempted to explain this shrinkage by the accumulation of vacancies and di-vacancies in the matrix. In metals under irradiation, during vacancy and vacancy cluster accumulation, however, interstitial clusters can grow larger [25]. Romano *et al*. [24] attempted to explain their results on the basis of point defect reactions. The disappearance of initially-formed {113} clusters and the formation of very small point defect clusters close to a surface of Fz-Si which was covered by an $Si_3N_4$ film was also observed by Fedina *et al*.[26]. They concluded that accumulated free vacancies in Fz-Si dissolved the nuclei of interstitial clusters.

Previous studies, however, did not consider the effect of impurities on the shrinkage of interstitial clusters. As it is generally accepted that impurities play a role in the growth of defect clusters [8, 17, 19-22], one could expect them to also have a role in the shrinkage of clusters. In this paper, we examine the behavior of irradiation-induced interstitial clusters on {113} planes under various irradiation conditions by HVEM. We then propose a model of the growth and shrinkage of clusters that includes the effects of impurities. A reaction kinetics analysis of point defects and impurities during irradiation is also performed to compare the model with experimental results.

## 2. Experimental

Fz non-doped (111) silicon wafers (< $10^{15}$ oxygen atoms /$cm^3$) and Cz non-doped (100) silicon wafers (about $10^{18}$ oxygen atoms /$cm^3$) were used in this experiment. A hollow was formed in the center of the disc, 3 mm in diameter, using a dimpler, and then the disc was chemically polished to create a small hole for electron microscopy. An impurity-doped Fz-Si specimen was prepared by heat treatment to compare the defect evolution with as-received Fz-Si. The heat treatment consisted of annealing the chemically-polished Fz-Si at 973 K for 5 hours in a vacuum of $1 \times 10^{-3}$ Pa. To avoid confusion, the heat-treated Fz-Si is referred to as HT-Fz-Si in this paper, and Fz-Si denotes the non-heat-treated Fz-Si. Electron irradiation was performed by an HVEM Hitachi H-1300 with an accelerating voltage of 1000 keV, and an electron intensity of $6 \times 10^{23}$ e/$m^2$·s unless specifically noted. The irradiation temperatures ranged from 573 K to 623 K. Detailed observations were made with a JEOL JEM-200CX after irradiation.

## 3. Results

### 3.1 Irradiation behavior of Fz-Si

An example of the irradiation behavior of Fz-Si is shown in Fig. 1. An incubation period of about 480 s was required to form clusters. All clusters were interstitial on [113] planes. The relatively long incubation period [9] can be explained by the differences in electron beam intensity and accelerating voltage. The implantation of gaseous atoms should be accelerated by increased intensity and energy of the electrons, as will be discussed in section 4.

### 3.2 Irradiation behavior of heat-treated Fz-Si and Cz-Si

The irradiation behavior of HT-Fz-Si was different from that of Fz-Si, as shown in Fig. 2. First, the {113} interstitial clusters nucleated without incubation. Then, they started to shrink under continuous irradiation. The clusters in the center of the beam, where the intensity was high, shrank faster than those off-center. At the farthest edge of the beam, where the intensity was quite low, clusters relatively unchanged. After 225 s, new clusters nucleated at the beam center, and these grew larger as the irradiation continued. The nature and shape of the clusters formed in these two stages were the same as those in Fz-Si (i.e., {113} interstitial clusters), but their spatial distributions differed. The clusters that formed without incubation were distributed homogeneously over the irradiated area, while the latter clusters existed only near the electron incident surface, similarly to those in Fz-Si. This behavior was the same in Cz-Si, and was similar to the observations of cluster formation made by Oshima *et al*. in Cz-Si [16] and by Hasebe *et al*. in carbon-doped Fz-Si [15]. Therefore, HT-Fz-Si was considered to contain sufficient impurities to form {113} interstitial clusters.

Figure 3 shows images taken before (left) and after (right) the shrinkage of clusters. The cross-sectional distribution of the clusters in a rectangular area was examined by stereo electron microscopy, and is shown in Fig. 4. During irradiation, the clusters began to shrink from the upper surface at the beam center. The broken lines in the figure indicate the boundary between disappearing clusters and the remaining clusters at each irradiation time. It is clear that the shrinkage of clusters was caused by not only an effect of homogeneous point defect reactions between vacancies and interstitials, but also by a direct effect of electron irradiation at the beam incident surface.

3.3 Directional dependence of growth and shrinkage of clusters on backside irradiated Fz-Si

Backside irradiation clearly showed the directional effects of electron irradiation on the growth behavior of clusters. First, Fz-Si was irradiated at 573 K for 1800 s to form well-developed {113} interstitial clusters near the beam incident surface (first-step irradiation). Then, by turning the specimen upside down, the same area was irradiated from the back side for 1260 s at the same temperature (second-step irradiation). Some clusters began to shrink immediately after the start of irradiation (Fig. 5), as was previously observed [23,24]. Figure 6 shows a cross-sectional view of the cluster shrinkage after backside irradiation for 155 s at 623 K. Two circles connected by a line indicate the upper and lower edges of clusters in the [110] direction. The clusters began to shrink along <110> from the area farthest from the surface. After second-step irradiation for 500 s, which corresponded to the incubation period of Fz-Si, new clusters nucleated and grew larger near the beam incident surface. The remaining clusters, those formed by the first-step irradiation that survived annihilation in the initial stage of the second-step irradiation, also started to grow, as can be observed in photos taken after 660, 1075, and 1260 s, which are shown in Fig. 5.

These results can be explained as follows. During the first step of irradiation, impurities were implanted by the electron irradiation, and accumulated near the electron incident surface, where clusters could nucleate and grow. With the start of backside irradiation, these clusters shrank because the impurities were no longer being supplied. After a long irradiation of 600 s, new clusters nucleated near the beam incident surface due to impurity implantation. Therefore, a continuous supply

of impurities is essential for the stable growth of clusters. A detailed discussion is presented in the following section.

The interstitial clusters observed in Fz-Si were on {113} planes, and were more elongated in the <110> direction than in the <332> direction, as shown in Fig. 7(a). The growth and shrinkage of clusters in these directions was compared between two typical clusters which were different orientation to the beam incident surface. Figure 7(a) shows the change in cluster size in the <110> and <332> directions during the first- and second-step (backside) irradiation. During the first-step irradiation, the clusters grew continuously in two directions, with a larger rate of growth in the <110> than <332> direction. During the back-side irradiation, however, the clusters continued growing in the <332> direction, but stopped growing in the <110> direction and began to shrink. The faster shrinkage in the [110] direction of the $(\bar{1}13)$ clusters than in the $[1\bar{1}0]$ direction of the (113) cluster is because one edge of the former cluster penetrated the interior, far from the surface, where the concentration of impurities was low during the first irradiation. Moreover, these impurities moved to the beam exit surface on bombardment by electrons. The same behavior was observed in HT-Fz-Si, where clusters first began to shrink in the region near the beam incident surface (Fig. 4).

3.4 Effect of electron irradiation intensity on cluster growth

Figure 8 shows the variation of cluster size in HT-Fz-Si under the electron irradiation at two different intensities, $6 \times 10^{23}$ and $2.6 \times 10^{22}$ e/m$^2$·s. Typical changes are shown in Fig. 9. Most of clusters which shrank under high intensity irradiation of $6 \times 10^{23}$ e/m$^2$·s grew at the lower intensity of $2.6 \times 10^{22}$ e/m$^2$·s. An acceleration in the rate of shrinkage at increasing irradiation intensity was reported

by Hasebe *et al*. [15]. This effect of beam intensity is expected from the results show in Figs. 2 and 3, where the clusters shrank only in the beam center and grew off-center in HT-Fz-Si. Some clusters in Fig. 9 which grew under high intensity irradiation were in the beam off center.

This explicitly demonstrates that cluster growth has a peculiar irradiation intensity dependence: the Frenkel pairs produced at an excessive rate do not contribute to the stable growth of {113} interstitial clusters in HT-Fz-Si or Cz-Si.

## 4. Discussion

### 4.1 Effect of impurities on cluster growth

The observed nucleation and growth of clusters cannot be explained solely in terms of the reaction between vacancies and interstitials. The effect of impurities is illustrated in Fig. 10. In Fz-Si, clusters cannot nucleate immediately after irradiation, because of a low concentration of impurities. During incubation, impurities are implanted from the surface by electron irradiation and accumulate near the electron incident surface regions. Then, the {113} interstitial clusters nucleate there.

In Cz-Si and HT-Fz-Si, there are pre-existing impurities in the bulk, and clusters can nucleate immediately upon irradiation. Under continuous irradiation, however, clusters begin to shrink. This is due to purification of the irradiated area by the absorption of impurities into clusters [22], and also by their escape to the surfaces [27]. In this condition, the concentration of impurities decreases to the level in Fz-Si, and clusters cannot grow larger, nor can they nucleate. If the irradiation continues, the implantation of impurities induces the nucleation of new clusters near the electron incident surface after a period of incubation. An incubation period of 225 s for the second nucleation of clusters in HT-Fz-Si (Fig. 2), shorter than the 480 s for

Fz-Si (Fig. 1), was due to the existence of residual impurities after the annihilation of clusters.

In the backside irradiation of Fz-Si (middle of Fig. 10), impurities are not supplied to clusters near the electron exit surface, which was the electron incident surface during the first irradiation. Without further supply of impurities by implantation, defects begin to shrink. New clusters then nucleate near the electron incident surface after the incubation period. The relationship between cluster growth and the concentration of impurities is discussed in the next section.

4.2 Mechanism of cluster growth

In this section, a simple model of the growth of {113} interstitial clusters in the presence of impurities is proposed. The irradiation conditions required for the continuous growth of clusters is then considered. Normally, the growth of irradiation-induced interstitial clusters is caused by absorption of interstitials and vacancies. The kinetics of defect growth can be discussed in terms of the concentrations of interstitials $C_I$ and vacancies $C_V$. The change of cluster radius $R$ can thus be described as [28]

$$\frac{dR}{dt} = aZ_{IC}M_I C_I - aZ_{VC}M_V C_V , \quad (1)$$

where $a$ is the change of the cluster radius on absorption of a single point defect, $Z$ is the number of sites for the absorption of point defects to clusters, and $M$ is the number of jumps per unit time. The subscripts $I$, $V$, and $C$ denote interstitials, vacancies, and clusters, respectively. The first term and second term of the right side are the changes in cluster radius by the absorption of interstitials and vacancies,

respectively. Immediately after electron irradiation, the point defect concentrations attain their quasi-equilibrium states, and

$$M_I C_I = M_V C_V = \left( \frac{P M_V}{Z_{IC}} \right)^{1/2} \tag{2}$$

is established [25], where $P$ is the production rate of point defects. Then, Eq. (1) can re-written as

$$\frac{dR}{dt} = a M_I C_I \left( Z_{IC} - Z_{VC} \right) . \tag{3}$$

Under normal irradiation conditions, interstitial clusters can grow larger due to the bias effect of clusters, i.e., $Z_{IC}$ is slightly larger than $Z_{VC}$.[29]. For cluster growth in silicon, this condition is adopted. The existence of impurities is essential to the absorption of interstitial silicon. We assume that impurities play a role in binding interstitials into clusters. Clusters are thus composed of interstitial silicon and impurities, as pointed out by Aseev *et al*. [8]. When an interstitial silicon is absorbed at a site that is not near an impurity, the silicon is assumed to evaporate easily, and to not contribute to cluster growth. In other words, only interstitial silicon located near impurities in clusters is stable. On the other hand, the absorption of vacancies will shrink the clusters. In this model, cluster growth depends on the absorption rate of both interstitial silicon ($Z_{CL} M_I C_I$) and impurities ($Z_{OC} M_O C_O$), where $O$ denotes impurities.

The ratio of $\frac{Z_{OC} M_O C_O}{Z_{IC} M_I C_I}$ is an important parameter, and we assume a critical ratio $\alpha$ for the stable growth of clusters. When the ratio is larger than the ratio $\alpha$ (namely, sufficient impurities are absorbed into clusters), the interstitial silicon is

also absorbed stably into clusters. Inversely, when the ratio is smaller than $\alpha$, the lack of impurities prevents cluster growth, and the absorption of impurities becomes the rate controlling process. In this case, the growth rate of the cluster does not depend on $Z_{IC} M_I C_I$, but on $Z_{OC} M_O C_O$. Introducing $\alpha$ into the cluster growth, Eq. (1) can be re-written as

$$\frac{dR}{dt} = aZ_{IC} M_I C_I + aZ_{OC} M_O C_O - aZ_{VC} M_V C_V \qquad (\frac{Z_{OC} M_O C_O}{Z_{IC} M_I C_I} > \alpha) \tag{4}$$

$$\frac{dR}{dt} = \frac{aZ_{OC} M_O C_O}{\alpha} + aZ_{OC} M_O C_O - aZ_{VC} M_V C_V \qquad (\frac{Z_{OC} M_O C_O}{Z_{IC} M_I C_I} < \alpha). \tag{5}$$

As the clusters consist of a large amount of interstitial silicon and few impurities, the change in the cluster radius due to the absorption of impurities can be ignored. Then, by using Eq. (2), the above equations become

$$\frac{dR}{dt} = aM_I C_I (Z_{IC} - Z_{VC}) \qquad (\frac{Z_{OC} M_O C_O}{Z_{IC} M_I C_I} > \alpha) \tag{6}$$

$$\frac{dR}{dt} = \frac{aZ_{OC} M_O C_O}{\alpha} - aZ_{VC} M_V C_V \qquad (\frac{Z_{OC} M_O C_O}{Z_{IC} M_I C_I} < \alpha). \tag{7}$$

Variation in the growth rate of clusters is shown schematically in Fig. 11 as a function of $M_I C_I$ and $M_O C_O$. Based on the above rate equations, the experimentally determined beam intensity dependence of the defect growth behavior (shown in Figs. 8 and 9) can be understood as follows. For a low impurity concentration, $C_O = C_O^{(1)}$, as seen in Fig. 11. When the irradiation intensity is as high as $6 \times 10^{23}$ e/m$^2$·s, the rapid production of point defects *P* induces a higher interstitial concentration, $C_I = C_I^{(2)}$, as can be seen in Fig. 11 and from Eq. (2). The

smaller $\frac{Z_{OC} M_O C_O^{(1)}}{Z_{IC} M_I C_I^{(2)}}$ of less than $\alpha$ results in shrinkage of clusters by the excess absorption of vacancies (the case of Eq.(7)). Even if impurities are released from the shrinking clusters, their concentration in the matrix will not increase, due to their escape to sinks such as the specimen surfaces. When the irradiation intensity is as low as $2.6 \times 10^{22}$ e/m$^2$·s, the lower production rate of point defects *P*, i.e., $C_I = C_I^{(1)}$,leads to $\frac{Z_{OC} M_O C_O^{(1)}}{Z_{IC} M_I C_I^{(1)}} > \alpha$ , and the clusters can grow larger (the case of Eq. (6)).

If the impurity concentration is high, $C_O^{(2)}$ in Fig. 11, which is the initial condition of impurities in HT-Fz-Si and Cz-Si, clusters can nucleate and grow larger regardless of the irradiation intensity. But, after a decrease in impurities to $C_O^{(1)}$ by irradiation-induced purification, only in the weak beam intensity area, where $C_I = C_I^{(1)}$, can clusters grow, as can be seen in Figs. 2, 3, and 4.

Aseev *et al.* [18] assumed $Z_{IC} < Z_{VC}$ , in order to explain the absence of interstitial clusters in an area far from the surface in the steady state of a point defect reaction ( $M_I C_I = M_V C_V$ ). However, as clusters formed only at the electron incident surface [9], as illustrated in Fig. 10, this assumption cannot be accepted.

### 4.3. Amount of impurities in clusters

The effect of impurities on cluster growth is very important. The Cz-Si used in these experiments contained about $10^{18}$ oxygen atoms/cm$^3$ at maximum. The

maximum concentration of interstitials in the interstitial clusters in Cz-Si was estimated to be $2x10^{19}$ atoms/$cm^3$ at 573 K. So, one oxygen affects 20 silicon interstitials on average, and $\alpha$=0.05 in our model, assuming that all of the oxygen was taken into clusters and $Z_{IC}M_I$ was equal to $Z_{OC}M_O$.

A cluster of four interstitials has been proposed as a possible structure of self-interstitial clusters in silicon by Takeda *et al*. [30]. They showed that a cluster of five interstitials was unstable, and suggested that impurities play an important role in extending the cluster by breaking bonds and rebonding involving silicon interstitials. Aseev *et al*. estimated the ratio of silicon interstitials to impurities in the cluster to be 1:1 in 973 K irradiation [8]. Our value of $\alpha$=0.05, seems small, even though our irradiation temperature was 573 K. If interstitial clusters absorb impurities preferentially by an interaction between clusters and impurities, a small value of $\alpha$ can be explained. Further study of this concept is required.

## 5. Conclusion

The growth of {113} interstitial clusters following electron irradiation in Fz-Si, impurity-doped Fz-Si (HT-Fz-Si) and Cz-Si was studied. The conclusions are as follows: (1) {113} interstitial clusters in silicon cannot grow without a continuous supply of impurities during electron irradiation. This mechanism was confirmed by the shrinkage of clusters in Cz-Si, HT-Fz-Si, and Fz-Si re-irradiated after reversing the specimen**.** (2) a model, which introduces a role for impurities as a binder of silicon interstitials in the cluster, explains the growth and shrinkage behavior of clusters under electron irradiation at different intensities.

**Acknowledgement**

The authors wish to express their most sincere gratitude to the late Professor Michio Kiritani. Without his support, encouragement and physical insight, our work would not have been possible.

**References**

1. M. L. Ciurea, V. Iancu, S. Lazanu, A. M. Lepadatu, E. Rusnac and I. Stavarache, Romanian Rep. Phys., 60 (2008) p.735.
2. G. Thomas, Phil. Mag. **17** (1968) p. 1097.
3. E. Nes and J. Washburn, J. Appl. Phys. **42** (1971) p. 3559.
4. M. D. Matthews and S. T. Ashby, Phil. Mag. **39** (1973) p. 1313
5. H. Föll, Inst. Phys. Conf. Ser. 23, (1975) p. 233.
6. S. Furuno, K. Izui and H. Otsu, Jpn. J. Appl. Phys., 18 (1979) p. 203.
7. I. G. Salisbury and M. H. Loretto, Phil. Mag. **39** (1979) p. 317.
8. A. L. Aseev, V. V. Bolotov, L. S. Smirnov and S. I. Stenin, Soviet Phys. Semicond., **13** (1979) p. 764.
9. H. Asahi, R. Oshima and F. E. Fujita, Inst. Phys. Conf. Ser. 59 (1981) p. 455.
10. S. Takeda, Jpn. J. Appl. Phys. **30** (1991) L639.
11. M. Kohyama and S. Takeda, Phys. Rev. B46 (1992) p. 12305
12. M. Kohyama and S. Takeda, Phys. Rev. B51 (1995) p. 13111
13. J.P. Goss, T. A. G. Eberlein, R. Jones, N. Pinho, A.T. Blumenau, T. Frauenheim, P. R. Briddon and S. Öberg, J. Phys. Condens. Matter 14 (2002) p. 12843.
14. S. Takeda, Microscopy Res. Tech., 40 (1998) p. 313.
15. M. Hasebe, R. Oshima and F. E. Fujita, Jpn. J. Appl. Phys., 25 (1986) p. 159

16. R. Oshima and G. C. Hua, Ultramicroscopy 39 (1995) p. 160.

17. P Werner, M. Reiche and J. Heydenreich, Inst. Phys. Conf. Ser. 134 (1993) p. 37.

18. A. L. Aseev, L. I. Fedina, D. Hoehl and H. Bartsch, Clusters of Interstitial Atoms in Silicon and Germaium (Berlin: Akademie Verlag, 1994)

19. S. Takeda, Inst. Phys. Conf. Ser. 157 (1997) p. 25.

20. S. Takeda, K. Koto, M. Hirata, T. Kuno, S. Iijima and T. Ichihashi, Materials science Forum, 258-263 (1997) p. 553.

21. K. Kodo, S. Takeda, T. Ichihashi and S. Iijima, Appl. Phys. Lett., 71 (1997) p. 1661.

22. A. R. bean, R. C. Newman and R. S. smith, J. Phys. Chem. Solid. 31 (1970) p. 739

23. G. C. Hua, R. Oshima and F. E. Fujita, J. Mater. Sci. **25** (1990) p. 328.

24. L. Romano and J. Vanhellemont, Mater. Sci. forum, 83-87 (1992) p. 303

25. N. Yoshida and M. Kiritani, J. Phys. Soc. Japan, 35, (1973) p. 1418.

26. L. Fedina, J. Van Landuyt, J. Vanhellemont and A. L. Assev, Nucl. Inst. Meth. Phys Res., B112 (1996) p. 133.

27. M. Kiritani, K. Urban and N. Yoshida, Rad. Effe. 61 (1982) p. 117.

28. M. Kiritani, N. Yoshida, H. Takata and Y. Maehara, J. Phys. Soc. Japan, **38**, (1975) p. 1677.

29. P.T. Heald, Phil. Mag. ,31 (1975) p. 551.

30. S. Takeda, N. Arai and J. Yamasaki, Mater. Sci. Forum, 258-263 (1997) p. 535.

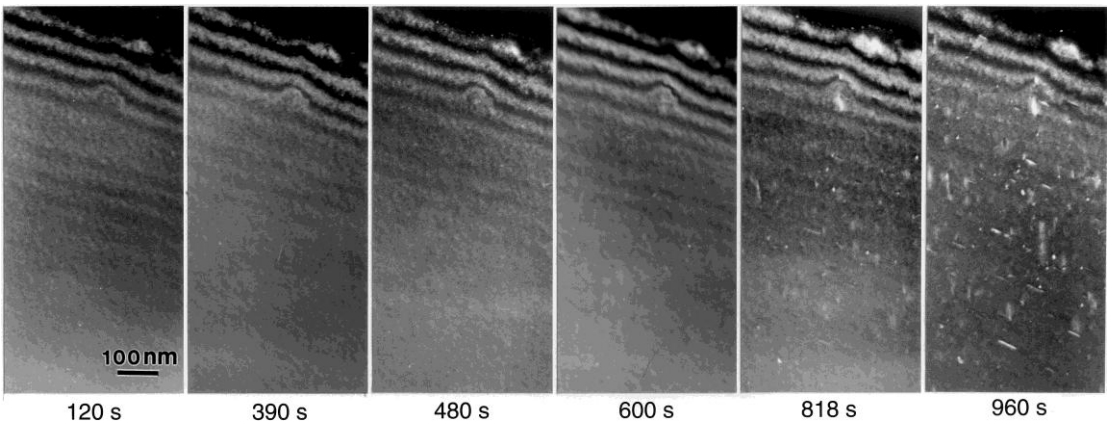


Fig. 1 Growth of {113} interstitial clusters in Fz-Si at 573 K under HVEM irradiation, 1 MeV and $6 \times 10^{23}$ e/m$^2$·s. Irradiation time is shown under each micrograph.

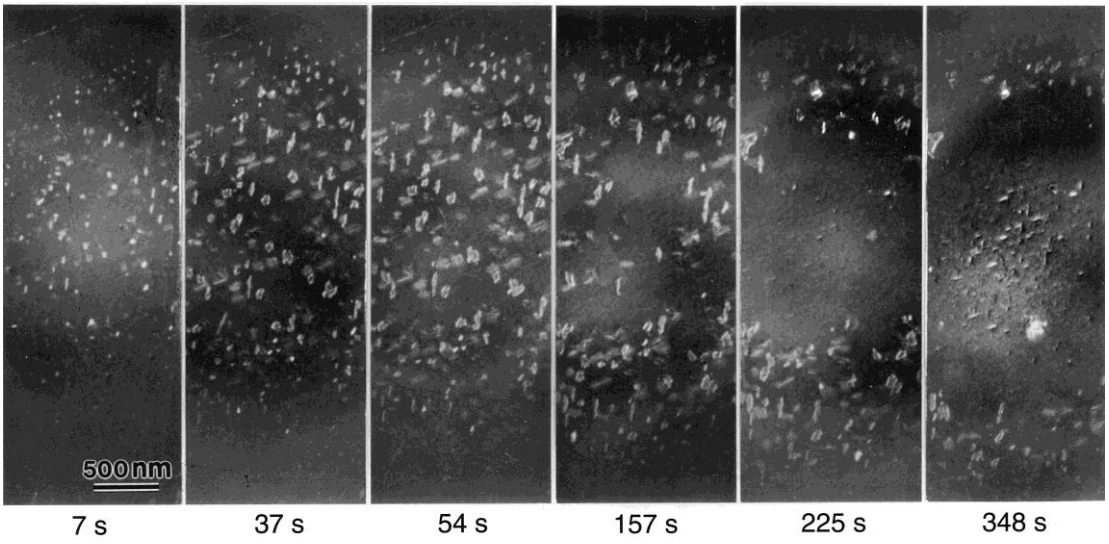


Fig. 2 Growth and shrinkage of {113} interstitial clusters in HT-Fz-Si at 573 K under HVEM irradiation, 1 MeV and $6 \times 10^{23}$ e/m$^2$·s. Irradiation time is shown under each micrograph.

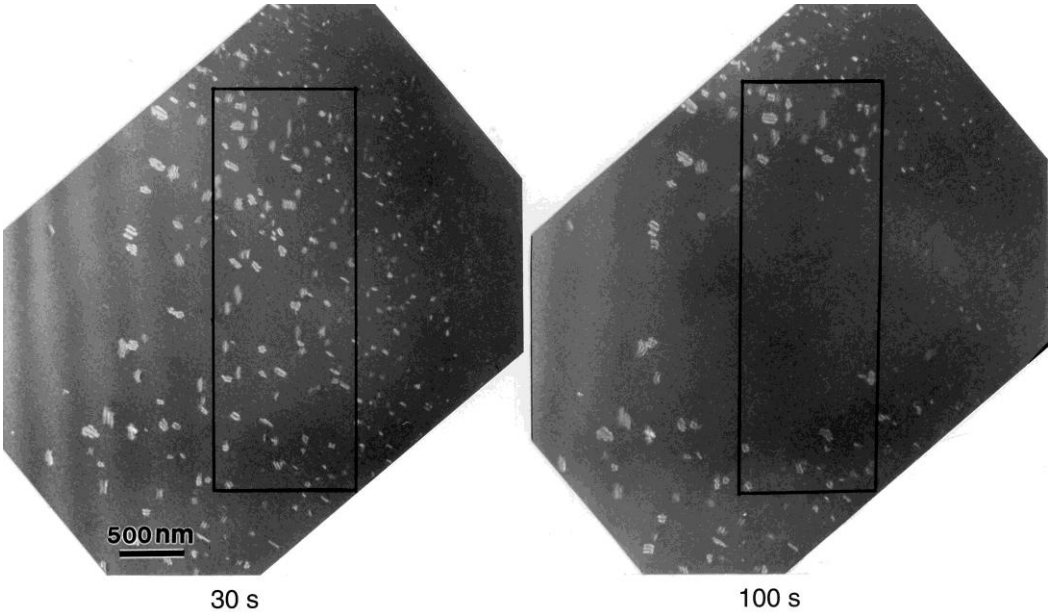


Fig. 3 Comparison of interstitial {113} clusters in HT-Fz-Si after irradiation for 30 s and 100 s at 623 K under HVEM irradiation, 1 MeV and $6 \times 10^{23}$ e/m$^2$·s.

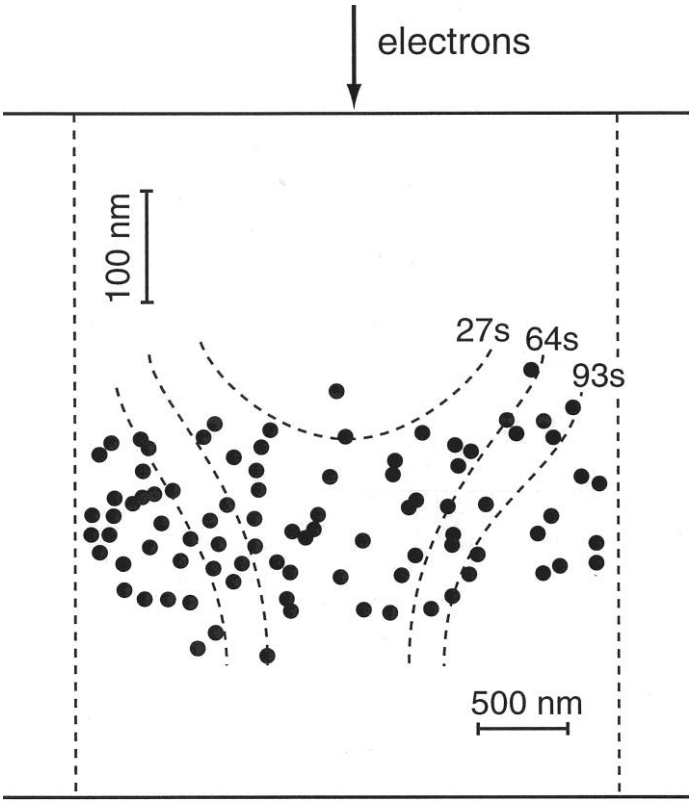


Fig. 4 Cross-sectional view of shrinkage behavior of {113} interstitial clusters in HT-Fz-Si at 623 K under HVEM irradiation, 1 MeV and $6 \times 10^{23}$ e/m$^2$·s. Each broken line shows the boundary where clusters remained at the irradiation time indicated.

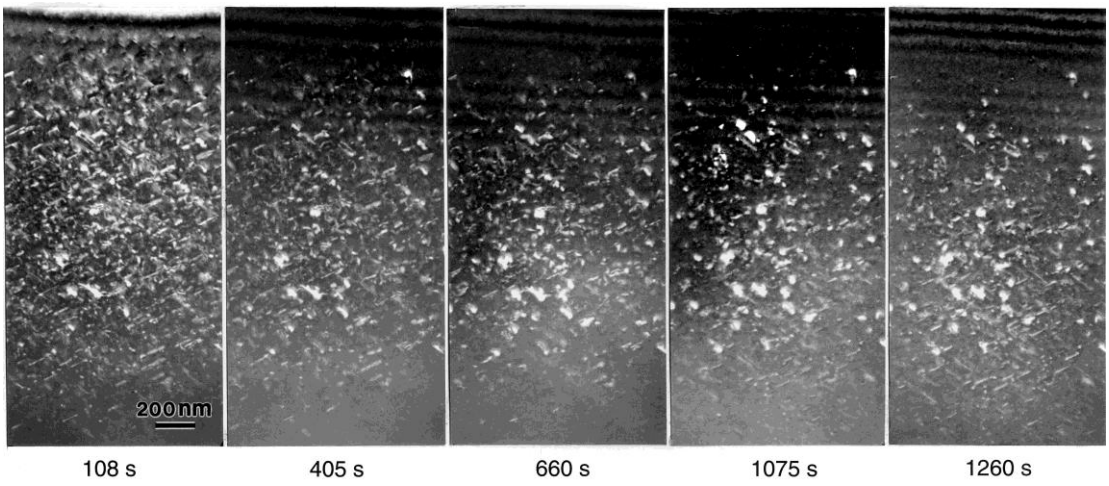


Fig. 5 Growth and shrinkage of {113} interstitial clusters in Fz-Si in two-step irradiation at 623 K under HVEM irradiation. First-step irradiation was for 1800 s. Second-step irradiation from the back side was conducted for the time indicated below each figure at $6 \times 10^{23}$ e/m$^2$·s.

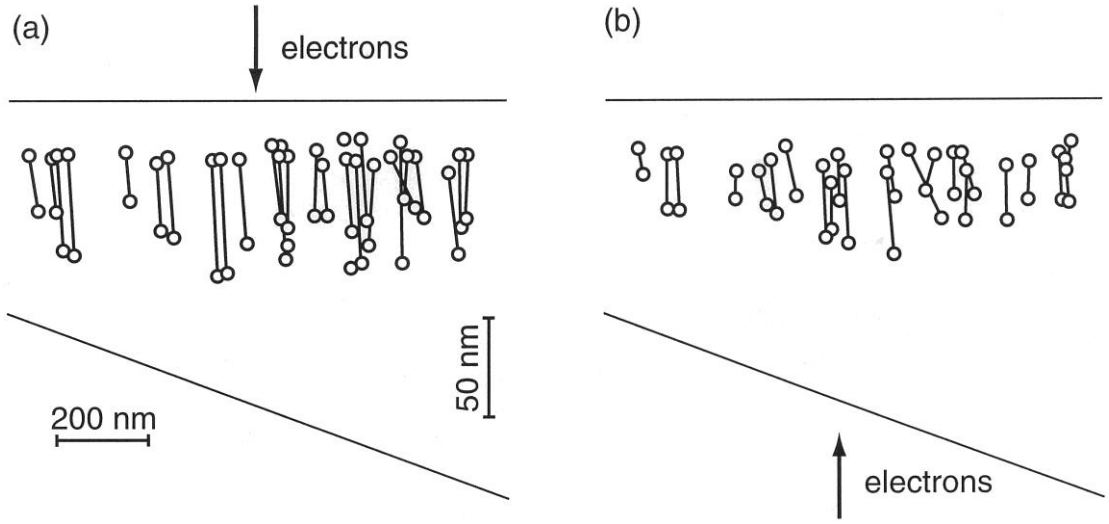


Fig. 6 Cross-sectional view of growth and shrinkage of {113} interstitial clusters in Fz-Si. First-step irradiation for 1800 s and second-step irradiation from the back side after turning the specimen upside down for 155 s (b). Both irradiations were at 623 K and $6 \times 10^{23}$ e/m$^2$ s.

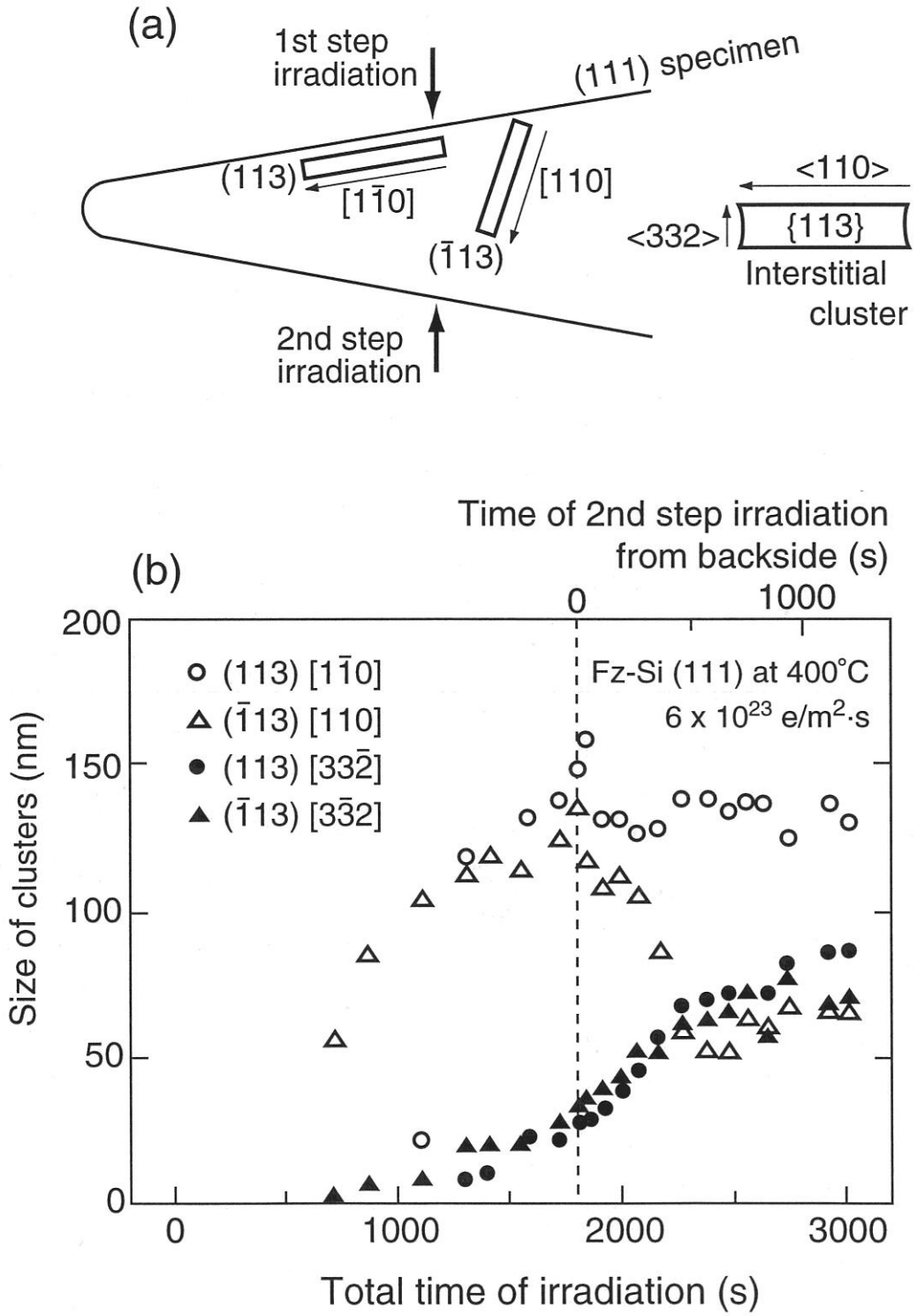


Fig. 7 Schematic illustration of specimen orientation and growth direction of {113} interstitial clusters (a) and the measured change in size of the clusters in Fz-Si during two-step irradiation (b). First-step irradiation was for 1800 s. Second-step irradiation was from the back side. Both irradiations were at 673 K and $6 \times 10^{23}$ e/m$^2$ s.

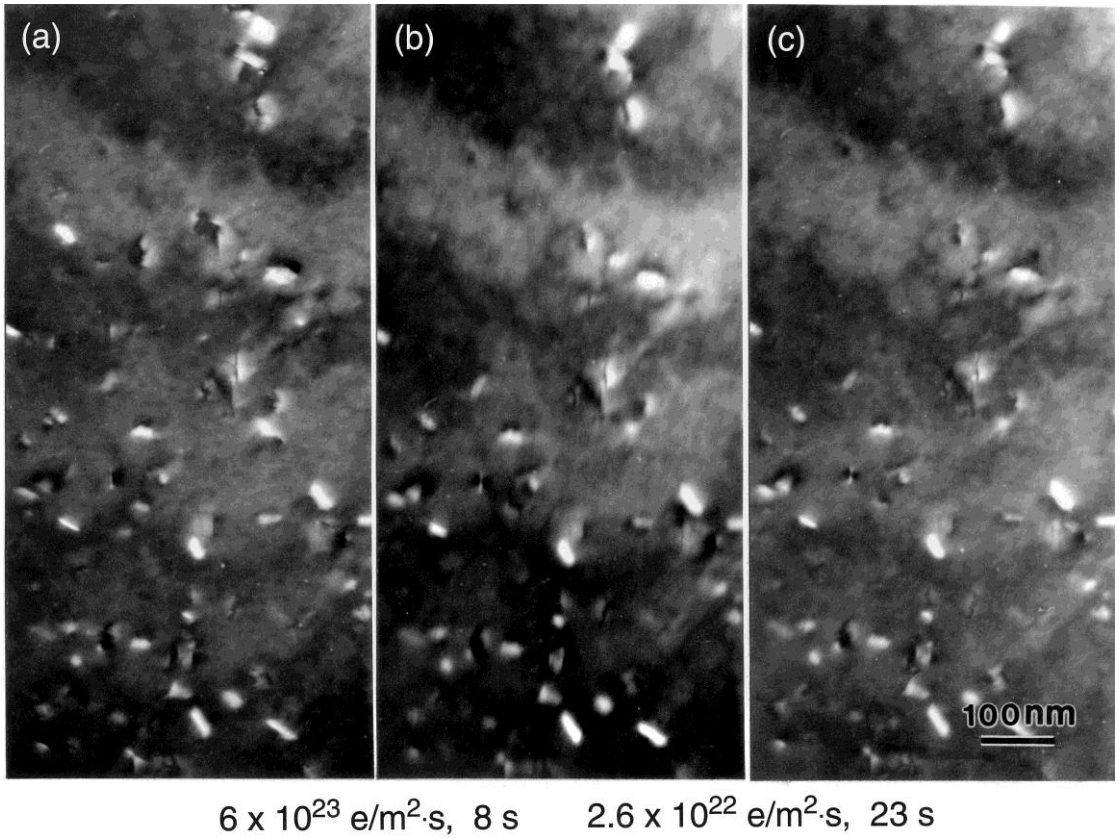


Fig. 8 Growth and shrinkage of {113} interstitial clusters in HT-Fz-Si at two different irradiation intensities at 573 K. (a) clusters introduced by irradiation for 30 s at a high beam intensity of $6 \times 10^{23}$ e/m$^2$ s, (b) after irradiation for 8 s at the same intensity, and (c) after irradiation for 23 s at a low intensity of $2.6 \times 10^{22}$ e/m$^2$ s.

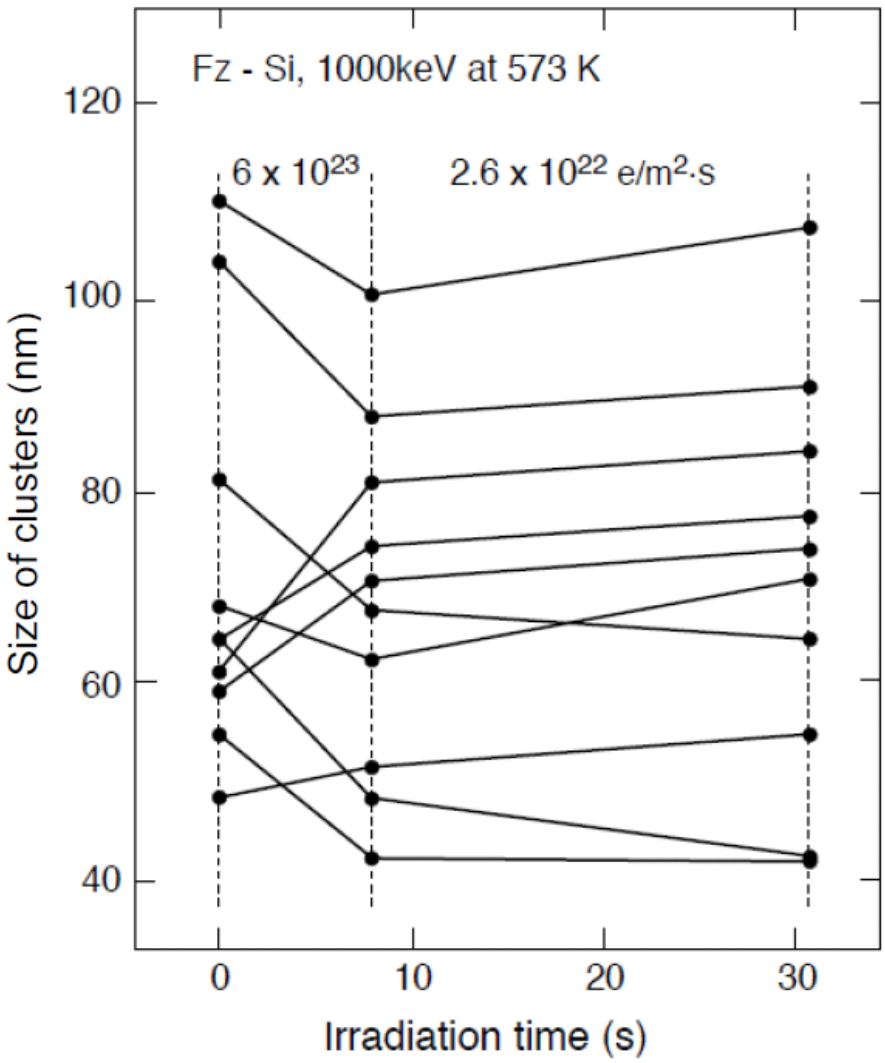


Fig. 9 Measured change in the size of {113} interstitial clusters in HT-Fz-Si at two different electron intensities.

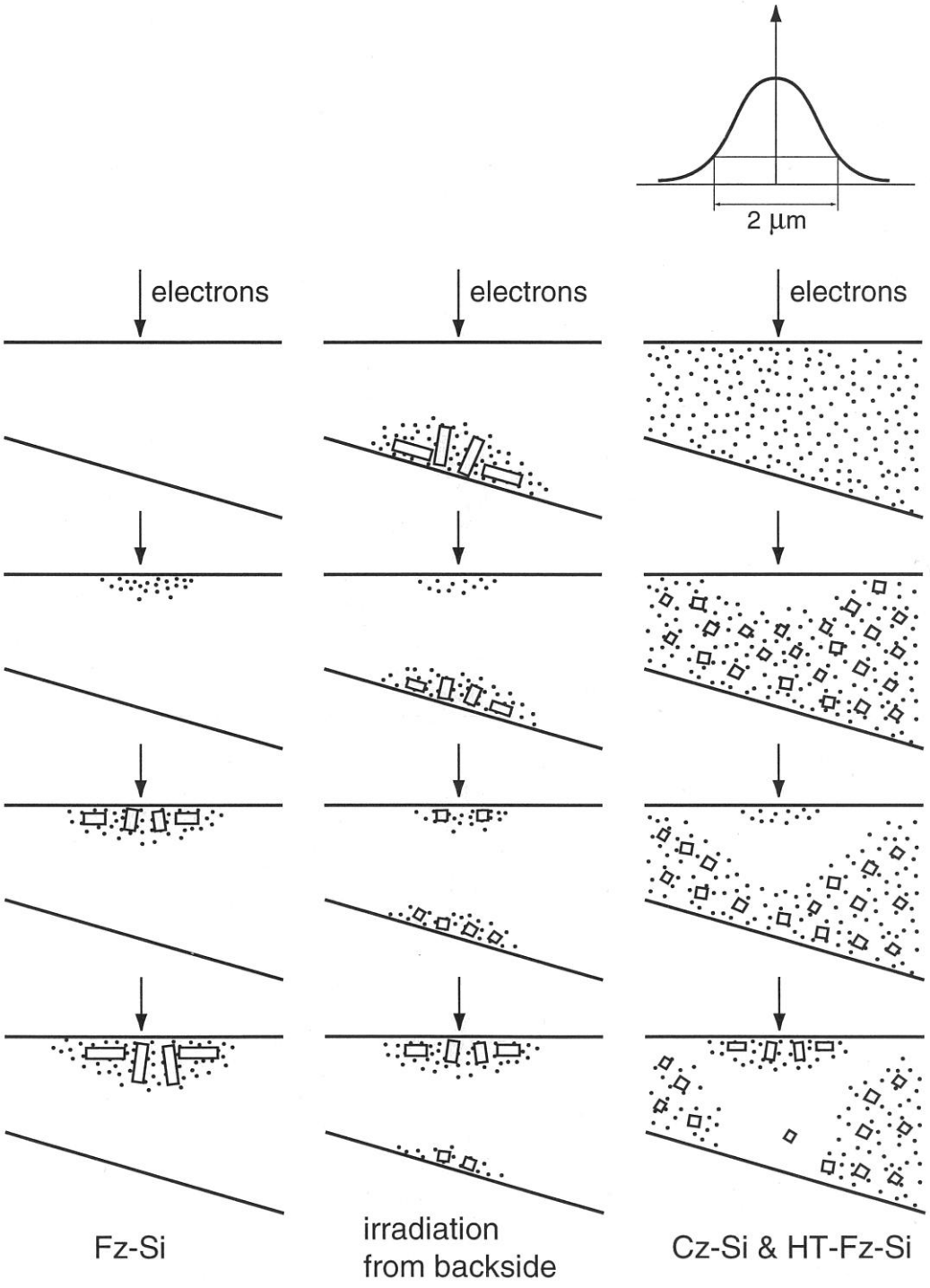


Fig. 10 Schematic illustration of growth and shrinkage behavior of {113} interstitial clusters in Fz-Si (left), backside irradiation of Fz-Si (middle), and HT-Fz-Si and Cz-Si (right). The black dots and rectangles represent impurities and interstitial clusters, respectively.

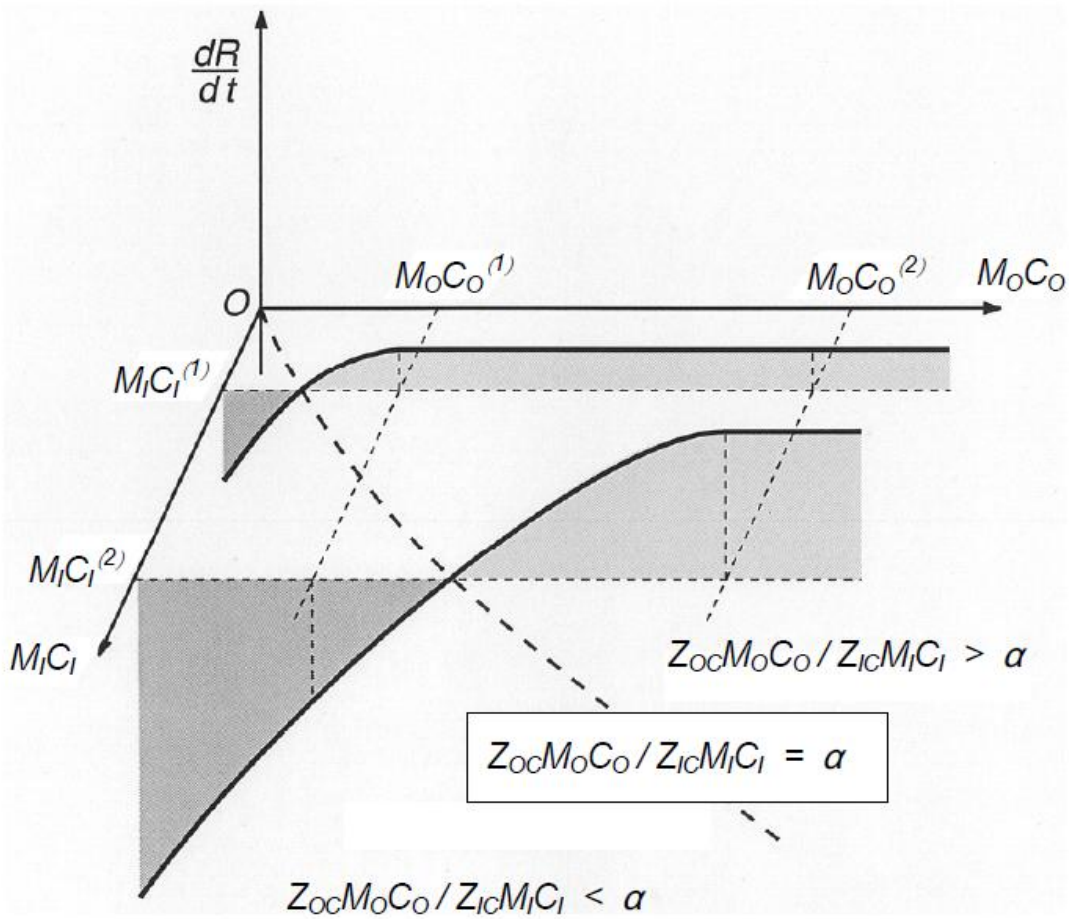


Fig. 11 Schematic illustration of the growth rate of {113} interstitial clusters *dR/dt* as functions of migration efficiency for silicon interstitials $M_IC_I$ and impurities $M_OC_O$.